



Lattice Boltzmann Method Application on Headwater at Lata Kinjang Waterfall, Malaysia

S. H. Shafiai^a, F. N. Sabri^a, A. Gohari^{*a}, H. Liu^b, Y. J. Wei^a

^a Civil and Environmental Engineering Department, Universiti Teknologi PETRONAS, Perak, Malaysia

^b School of Environment, Beijing Normal University, Bei Tai Ping Zhuang, Haidian Qu, Beijing Shi, China

PAPER INFO

Paper history:

Received 23 January 2020

Received in revised form 18 February 2020

Accepted 19 March 2020

Keywords:

Headwater Accident

Lattice Boltzmann Method

Shallow Water Flow with Turbulence

Modeling

Simulation

Two-dimensional

ABSTRACT

Headwater accident is a natural phenomenon that occurs in every flow channel, resulting in tremendous incidents that involve vulnerable lives and destruction of its surroundings. This study focuses on simulation of potential headwater accidents at Lata Kinjang waterfall (Perak, Malaysia) with the aim of understanding the behavior of headwater accidents from the hydraulic aspect. By deploying the Lattice Boltzmann Method (LBM) for Shallow Water Flow with Turbulence Modeling (LABSWETM), a two-dimensional simulation was carried out to investigate the headwater condition of the study area. The outputs from the LABSWETM model simulation were presented in terms of water height progression and velocity profile. The water-height results showed a decrease in water level within the flow channel and an increase in downstream, while the velocity-profile results revealed an increase in velocity at downstream. Thus, under current hydraulic conditions, Lata Kinjang waterfall has a high potential for the occurrence of headwater accidents. Nonetheless, this study provide suggestions to mitigate the phenomenon efficiently.

doi: 10.5829/ije.2020.33.05b.07

NOMENCLATURE

f_{α}	Particle distribution function	g	Gravity (m/s ²)
\hat{f}_{α}	Value of f_{α} before the streaming	h	Coefficient
Δx	Lattice size in x-direction	L_x	No. of lattices in x-direction
Δy	Lattice size in y-direction	L_y	No. of lattices in y-direction
Δt	Time step	Greek Symbols	
F_i	Component of the force in i direction	τ	Lattice relaxation time
e_{α}	Velocity vector of a particle in the α link	ρ	Density (kg/m ³)
N_{α}	constant	ν	Kinematic viscosity (m ² /s)
f_{α}^{eq}	Local equilibrium distribution function	Subscripts	
Ω_{α}	collision operator	i & j	Space direction indices

1. INTRODUCTION

Streams and rivers can be represented in hierarchical networks including small and large branches of water. Large branches are formed by joining a variety of small branches since the water travels downhill. The headwater stream is the finest branch of such networks [1]. Headwater streams are more hydraulically connected to

hillslope and groundwater processes than larger streams [2,3]. Headwater accidents are frequently defined as the abrupt flow of water in huge volumes from the upstream of a river or from waterfall to the main river stream. The headwater is generally attributable to the incidence of heavy rainfall in upstream of the river. Initially, the flow of vast amounts of water is hindered by the presence of objects such as rocks and logs of wood in upstream of a

*Corresponding Author Email: adel.gohari@gmail.com (A. Gohari)

river. However, heavy rain produces large volumes of water with enough impact to wash off the objects that hinder flow, and cause the water to surge from upstream to downstream.

The condition of headwater could cause the destruction of the riverbank, and endanger lives and properties. As reported [4], a group of 7 people were injured on a picnic trip in Lata Kinjang waterfall. The incident was due to the gushing water from the upstream of the waterfall (headwater). In a similar report, a 44-year old man was found drowned in Sungai Kenerong, Kota Bharu, also due to headwater accident [5]. This evidently shows the endangering impact of headwater on human lives. To mitigate this problem, the Malaysian government has announced the installation of a warning system to avert headwater accidents. However, the functionality and suitability of the warning system is yet to be ascertained, possibly due to limited studies on headwater conditions, particularly in terms of hydraulics. Moreover, headwater can also lead to flash floods which frequently occur on small headwater basin. Most flood incidents occur near a river or a stream with source of water being a heavy rainfall over a catchment area. Flash floods can lead to massive destruction of infrastructure, and cause mortal injuries to humans and animals [6]. The identification of high-risk areas with potential overflow is a significant measure in flood control [7]. Hence, computational studies on headwater accidents require the study of the behavior of headwater in terms of water height and velocity. The outcome of this study will help in determining the sections of Lata Kijang waterfall that pose high risks of being affected by headwater. This will aid the development of mitigation measures that can be implemented prior to headwater incidents, thereby lessening the adverse effects of headwater accidents.

Lata Kinjang waterfall is considered as one of the highest waterfalls in Malaysia which cascades down a steep 200-meter high-stretch of rocky slopes and surfaces. This accounts for its selection as a study area. It is located at Chenderiang, about 12km north of Tapah town, Perak state. The study area location and the headwater occurrence are shown in Figures 1 and 2, respectively.

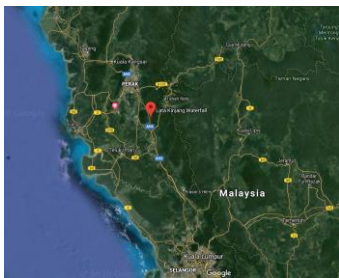


Figure 1. The location of Lata Kinjang waterfall in Malaysia



Figure 2. Normal water flow from upstream (left) and headwater accident (right)

Computational methods are defined as mathematical calculation models developed to study the behavior of a complex system. A number of computational studies have been conducted to model flow in a river system. For instance, Giertz et al. [8] simulated the hydrological processes in a headwater catchment in Benin using SIMULAT-H which is a semi-distributed hillslope version of the 1-D SVAT-model SIMULAT. Their simulation results of runoff generation processes were found to be consistent with field investigations. Voltz et al. [9] investigated riparian hydraulic gradients over three different time scales in two steep, forested, headwater catchments in Oregon to determine the potential controls of reach-scale valley slope and cross-sectional valley geometry. They discovered that steep headwater valley floors host extensive stream water exchange with very little change in the water table gradients over 3 orders of magnitude of stream discharge. Voeckler et al. [10] explored the potential contribution of deep groundwater recharge to the bedrock in a snowmelt-dominated headwater catchment in Okanagan Basin, British Columbia by using a coupled surface water-groundwater model. They reported a strong connection between the bedrock and the soils, particularly in the lower riparian zones of the headwater catchment. In addition, there are reasonable recharge and discharge zones during high- and low flow seasons. Kelleher et al. [11] confirmed the ability of the Distributed Hydrology Soil Vegetation Model (DHSVM) to model dominant controls on catchment response to hydrologic partitioning across five adjacent headwater sub-catchments. Niu et al. [12] utilized the Variable Infiltration Capacity (VIC) model combined with a routine scheme to investigate the multi-scale streamflow variability responses to the precipitation over 16 headwater catchments in the Pearl River basin, South China. Li et al. [13] developed a novel approach to estimate the Active Stream Network Lengths (ASNL), under different wetness conditions, of Sagehen Creek catchment by using streamflow recession analysis. Neupane et al. [14] predicted potential hydrologic changes in a Rocky Mountain headwater catchment by simulating water budgets of the Athabasca River using a calibrated version of the Soil and Water Assessment Tool (SWAT). The results of their simulation indicated that the hydrologic model is a valuable tool for assessing the effects of potential changes in temperature and

precipitation on hydrological processes in a basin. Allen et al. [15] investigated the relationship between stream width and abundance in headwater stream networks across North America and New Zealand. They have modeled stream widths by combining principles of conservation of mass, hydraulic resistance, downstream hydraulic geometry, and the natural variability of channel cross-sectional geometry. They inferred that stream widths in headwater networks have a lognormal distribution.

Among the computational methods, Computational Fluid Dynamic (CFD) modeling has been advanced and widely used as a tool for analyzing liquid flow since the early 20th century. CFD combines applied mathematics, physics concepts and calculation software to simulate gas or liquid flows. A viable substitute for CFD methods is the Lattice Boltzmann Method (LBM) which is a powerful computational tool for simulating different types of flows [16]. LBM is effective for simulating fluid flow within complex geometries and topologies. It is based on statistical physics, and is used to provide accurate description of fluid flow at microscopic level in an extremely simplified way, but a correct average description of fluid flow at the macroscopic level [17]. During the past decade, LBM has attracted widespread interest of researchers in fluid problems, and is extensively used for modeling both single-phase and multiphase fluids [14]. Compared to classic CFD methods, the LBM is considered a relatively simple method and it helps researchers to solve many types of complex fluid transport phenomena coupled with electrokinetics, magnetics, thermodynamics, etc. However, the main limitation of LBM is its memory costs [18].

Several studies have implemented LBM to investigate fluid flow. Hedjripour et al. [19] applied one-dimensional LBM techniques in the assessment of flow field patterns and flow characteristics such as depth, velocity etc., with a focus on shallow water problems within the subcritical and supercritical regimes. The model displayed good to excellent conformity with those from analytic solutions or other models over a range of steady-state and unsteady problems. Dolanský et al. [20] developed a three-dimensional LBM-based simulation to investigate the motion of particles in a pipe with a rough bed. Their results confirm simulation that LBM is a useful tool for hydrodynamic applications. Several studies have been performed on the application of LBM in Shallow water flow. Mousavi et al. [21] implemented LBM to simulate the deformation and breakup of a falling droplet under the gravity force. They concluded that increasing the Ohnesorge number mainly causes a shift in the boundary between the different breakup modes to higher Eotvos number. Sheikholeslami and Ashorynejad, [22] applied LBM to examine the natural convection flow of nanofluids in a concentric annulus. They found that the improvement of heat transfer is highly dependent on the

type of nanofluid. A detailed review of the application of LBM in shallow water flow is provided in recent and relevant studies [23-30].

Despite the relatively large number of researches related to headwater studies, emphasis has been placed on hydrology modeling with less consideration given to hydraulic aspects. The main objective of this study is to analyze the headwater accidents in terms of water height and velocity from upstream to downstream along Lata Kinjang waterfall by using the two-dimensional LBM for shallow water flow integrated with turbulence modeling (LABSWETM). LABSWETM, which stands for Lattice Boltzmann for Shallow Water Equation with Turbulence Modeling, is a numerical model developed based on Lattice Boltzmann method. This LABSWETM model is written in code form in MATLAB software. The model was developed by Zhou [31] in 2004 and has been widely used to solve complex hydrodynamic problems involving turbulent water flow. In this study, the LABSWETM was modified in terms of channel profile, bed slope, boundary condition, and headwater condition to simulate the phenomena in Lata Kinjang waterfall.

This paper provides a theoretical background of the LBM. The model was implemented on turbulent flow in Lata Kinjang waterfall, followed by validation of data, rendering of results and suggestion of solutions. Conclusions were then drawn from the results.

2. THEORETICAL BACKGROUND OF LBM

The LBM is a numerical computational method for the simulation of various types of flows within complex geometries. The LBM is classified as a mesoscopic scale simulation that considers the behavior of a collection of particles as a single unit. Zhou [31] reported that the LBM is an integration of Lattice Gas Automata (LGA) which solves the difficulties of the latter. In terms of fundamentals, the particle distribution functions replaced the Boolean variable from LGA equation [31], as presented below:

$$f_{\alpha}(x + e_{\alpha}\Delta t, t + \Delta t) = \hat{f}_{\alpha}(x, t) + \frac{\Delta t}{N_{\alpha}e^2} e_{\alpha i} F_i(x, t) \quad (1)$$

where f_{α} is the particle distribution function; $e = \Delta x/\Delta t$, where Δx is the lattice size and Δt is the time step. N_{α} is a constant determined by Equation (2) [32].

$$N_{\alpha} = \frac{1}{e^2} \sum_{\alpha} e_{\alpha x} e_{\alpha x} = \frac{1}{e^2} \sum_{\alpha} e_{\alpha y} e_{\alpha y} \quad (2)$$

Basically, the LBM is modeled based on three main components, which are the lattice pattern, Lattice Boltzmann equation, and the distribution function model. Lattice pattern plays a vital role in the LBM as it serves two functions: displaying the grid points as well as indicating the motion of particles [31]. There are two types of 2-dimensional lattice patterns, which are square

lattice and hexagonal lattice as shown in Figures 3 and 4, respectively. The type of lattice pattern is dependent on the speed of the particle at the lattice node. The 9-speed square lattice and 7-speed hexagonal lattice both have enough lattice symmetry and show adequate results in numerical studies.

The fluid particles move individually on a lattice unit through the path of the specified link with its velocity. For a 9-speed square lattice unit, the velocity of the particles is determined by Equation (3). The LBM comprises two important steps that include streaming and collision [31, 32]. These steps are all expressed in Equation (4) [31].

$$e_\alpha = \begin{cases} (0,0), & \alpha = 0, \\ e \left[\cos \frac{(\alpha-1)\pi}{4}, \sin \frac{(\alpha-1)\pi}{4} \right], & \alpha = 1,3,5,7, \\ \sqrt{2}e \left[\cos \frac{(\alpha-1)\pi}{4}, \sin \frac{(\alpha-1)\pi}{4} \right], & \alpha = 2,4,6,8. \end{cases} \quad (3)$$

$$\underbrace{f_i(\vec{x} + \vec{e}_i \Delta t, t + \Delta t) - f_i(\vec{x}, t)}_{\text{Streaming}} = - \underbrace{\frac{[f_i(\vec{x}, t) - f_i^{eq}(\vec{x}, t)]}{\tau}}_{\text{Collision}} \quad (4)$$

The streaming step, which is articulated in Equation (1), occurs when the particles are displaced to neighboring lattice points along the specified link path in its velocity. In the collision step, the particles arriving at the points interact with one another and change their velocity directions according to scattering rules, which is expressed as Equation (5) [31].

$$f'_\alpha(x, t) = f_\alpha(x, t) + \Omega_\alpha [f(x, t)] \quad (5)$$

where Ω_α is the collision operator which controls the speed of change in f_α during the collision.

To solve the shallow water condition, Equation (6) was derived and used in Lattice Boltzmann equation as suggested in an earlier study [31].

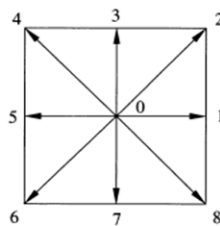


Figure 3. 9-speed square lattice [31]

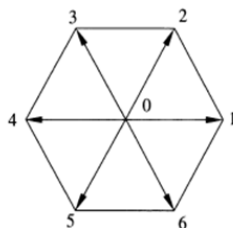


Figure 4. 7-speed hexagonal lattice [31]

$$f_\alpha^{eq} = \begin{cases} h - \frac{5gh^2}{6e^2} - \frac{2h}{3e^2} u_i u_j, & \alpha = 0, \\ \frac{gh^2}{6e^2} + \frac{h}{3e^2} e_{\alpha i} u_i + \frac{h}{2e^4} e_{\alpha i} e_{\alpha j} u_i u_j - \frac{h}{6e^2} u_i u_j, & \alpha = 1,3,5,7, \\ \frac{gh^2}{24e^2} + \frac{h}{12e^2} e_{\alpha i} u_i + \frac{h}{8e^4} e_{\alpha i} e_{\alpha j} u_i u_j - \frac{h}{24e^2} u_i u_j, & \alpha = 2,4,6,8. \end{cases} \quad (6)$$

$$f_\alpha(x + e_\alpha \Delta t, t + \Delta t) - f_\alpha(x, t) = -\frac{1}{\tau} (f_\alpha - f_\alpha^{eq}) + \frac{\Delta t}{6e^2} e_{\alpha i} F_i \quad (7)$$

According to Zhou [27], the LBM is indeed a useful and efficient computational fluid dynamics technique to simulate flow based on several advantages that include: ease of programming as it utilizes only simple arithmetic calculations; only the microscopic distribution is unknown, which is a direct and less complicated approach than the traditional methods; ideal for parallel computations since the current value of distribution function only depends on previous conditions; simple implementation of boundary conditions which makes it suitable for flows in complex geometry, and it enables unhindered simulation of complex flows.

3. METHODOLOGY

In this research, the LABSWE™ was implemented to simulate the incidence of headwater at the Lata Kinjang waterfall. The LABSWE™ model was modified in terms of channel profile, bed slope, boundary condition, and headwater condition to enable the simulation of turbulence flow at Lata Kinjang waterfall. Figure 4 presents a flowchart of this research. The simulation procedures are designed in line with previous reports [31]. The details of each task mentioned in the flowchart are explained in the following subsection.

3. 1. Channel Profile The channel profile of the Lata Kinjang waterfall is synchronized with the LBM model by through the combination of the LABSWE™ model with AutoCAD drawing of the channel profile, as shown in Figure 5.

The sketch was then converted into JPEG file with a pixel size of 559 x 109. In order to display the channel profile as sketched, the channel dimension was scaled down to 64% of the original sketch in terms of length and width in the LABSWE™ model. Using the masking function in MATLAB, the channel sketch was successfully masked into the LABSWE™ model. The sketch is represented by a binary mask where ‘0’ and ‘1’ indicate the channel bed and solids beside the channel, respectively. The top view and 3-dimensional view in MATLAB are displayed in Figures 6 and 7, respectively.

3. 2. Bed Slope To obtain a realistic output from the study, the bed slope of the channel was considered in the simulation model. Figure 8 shows the actual elevation and slope of Lata Kinjang waterfall. The bed slope profile was

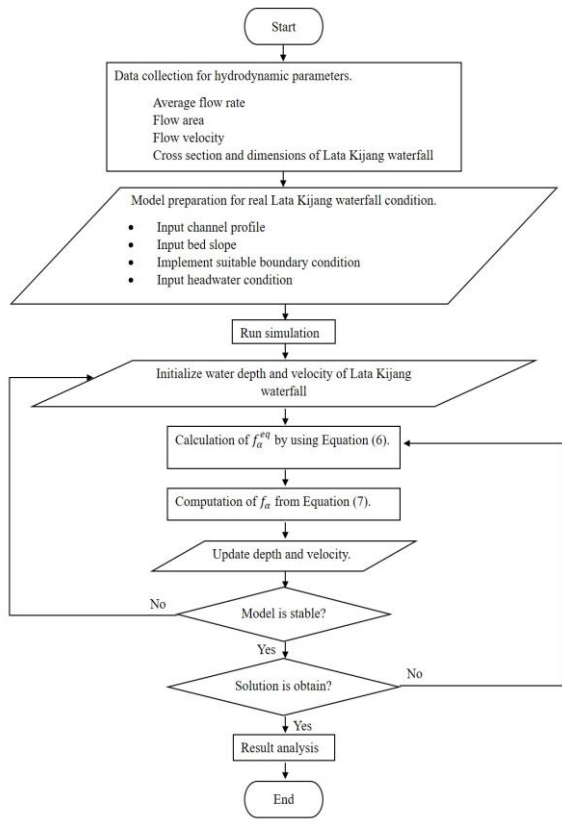


Figure 4. Flowchart of research methodology

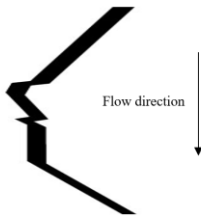


Figure 5. Sketch of the channel profile of Lata Kijang waterfall

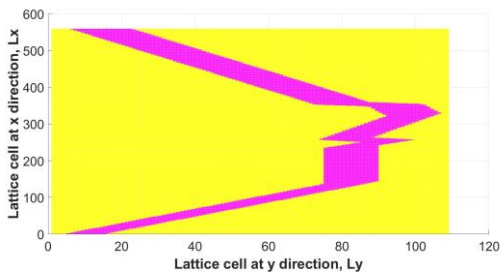


Figure 6. Top view of channel profile in LABSWE™

divided into 5 sections with each section having a different value for slope. The value of the gradient is shown in Table 1.

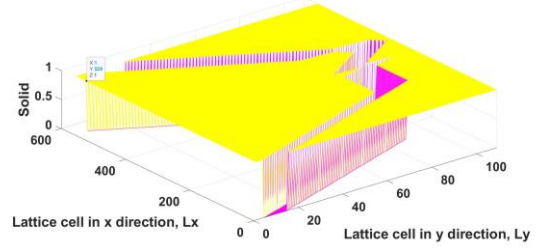


Figure 7. 3-D view of channel profile in LABSWE™

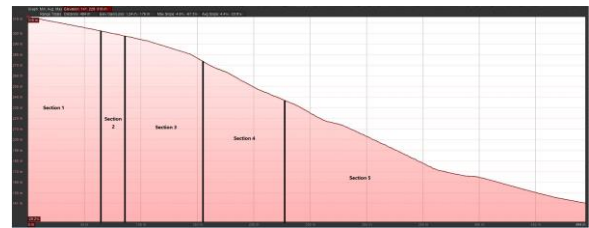


Figure 8. Elevation and slope profile of Lata Kijang waterfall

TABLE 1. Slopes of Lata Kijang Waterfall

Section	Location	Slope
1	Head to 65 meters from head	-0.21818
2	65 meters to 85 meters from head	-0.35294
3	85 meters to 155 meters from head	-0.52066
4	155 meters to 227 meters from head	-0.42149
5	227 meters from head to outlet	-0.238095

3. 3. Boundary Condition

According to Zhou [31], the boundary condition of the channel must be determined to provide a solution for turbulent water flow in shallow water conditions. In this simulation model, the no-slip boundary condition is specified between the solids and water flow. Day [33] mentioned that the no-slip boundary condition is applied where the fluid velocity along the channel boundary is the same as the solid boundaries. Therefore, it is assumed that the velocity of fluid will be zero with respect to the boundary. However, based on the channel profile of Lata Kijang waterfall in LABSWE™ model, there are a few sharp corners, which are observed in Figure 9.

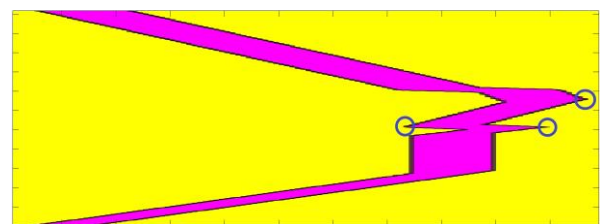


Figure 9. Sharp corners in channel profile

Due to the inability of the LABSWE™ model to determine the water depth when water heights from two directions interact with each other, corner treatment has to be done for the sharp corners. The corner treatment is done by specifying the unknown distribution function of the lattice pattern from the neighboring cell of the boundary cell to a known distribution function that is opposite the unknown distribution function. For example, in the case of Figure 10, the unknown distribution functions (f7, f6, and f8) are assigned to be equal to the known distribution functions (f3, f4 and f2) [31]. With the application of corner treatment, the simulation of headwater incidence at Lata Kinjang waterfall is more stable and accurate.

3. 4. Headwater Condition Given the similarity of the headwater and dam-break flow conditions, the same approach of initializing the simulation was introduced in this study. The channel is separated into two sides by assigning different water depths during the initialization phase. The water depth along the channel of Lata Kinjang waterfall is shown in Figure 11. The headwater condition illustrates the scenario where the water initially retained in the basin by objects surges downstream due to the removal of the objects.

4. RESULTS AND DISCUSSION

For validation, the result of the model was compared with the most updated flow parameters (e.g. water depth of the

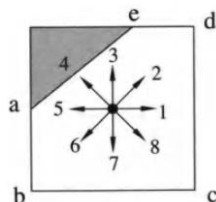


Figure 10. Example for corner treatment [31]

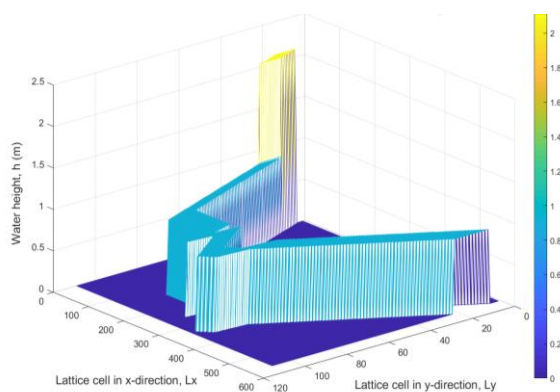


Figure 11. Headwater condition set-up

flow) of Lata Kinjang waterfall collected from the Department of Irrigation and Drainage (DID) Malaysia. For the simulation, a lattice cell of 559 x 109 was used. The validation was carried out on several hydrodynamic parameters from three different consecutive years (2015, 2016 and 2017). Using the trial and error method, time step (Δt) of 0.0005s and relaxation time (τ) of 1.0 with 25,000 iterations are determined to keep the turbulent flow model in steady-state flow.

The first validation was done using recent hydrodynamic input parameters from 2017 (See Table 2). The values for initial water depth (h) and initial flow velocity (u) were considered as 0.80176m and 0.744m/s, respectively. The initial water depth obtained from DID was plotted and compared with the water depth simulated from LABSWE™. The comparison of the output of the model at water depth of $L_x=378$ with the data collected from DID is shown in Figure 12.

TABLE 2. Input parameters for simulating water depth for year 2017

Parameters	Value
No. of lattices in x-direction, L_x	559
No. of lattices in y-direction, L_y	109
Initial water depth, h	0.80176m
Initial flow velocity, u	0.744m/s
Time step, Δt	0.0005s
Relaxation time, τ	1.0
Lattice size in x-direction, Δx	0.5m
Lattice size in y-direction, Δy	0.5m

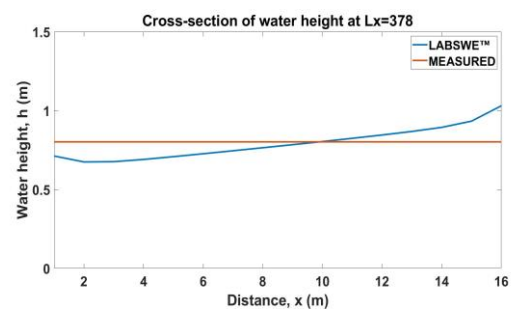
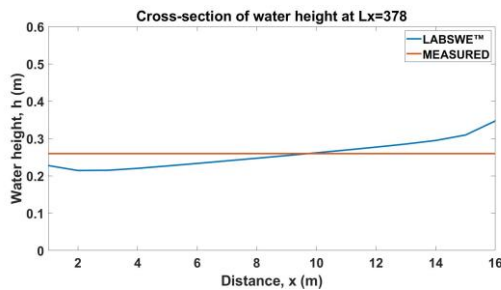


Figure 12. Cross-section of simulated against measured water depth for year 2017

The second validation was done using hydrodynamic input parameters from 2016 (See Table 3). The values for initial water depth (h) and initial flow velocity (u) were considered as 0.25952m and 0.456m/s, respectively. The initial water depth obtained from DID was plotted and compared with the water depth simulated from LABSWE™, as shown in Figure 13.

TABLE 3. Input parameters for simulating water depth for year 2016

Parameters	Value
No. of lattices in x-direction, L_x	559
No. of lattices in y-direction, L_y	109
Initial water depth, h	0.25952m
Initial flow velocity, u	0.456m/s
Time step, Δt	0.0005s
Relaxation time, τ	1.0
Lattice size in x-direction, Δx	0.5m
Lattice size in y-direction, Δy	0.5m

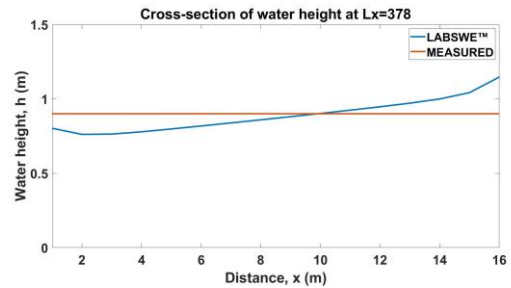
**Figure 13.** Cross-section of simulated against measured water depth for year 2016

The third validation was done using hydrodynamic input parameters from 2015 (See Table 4). The values for initial water depth (h) and initial flow velocity (u) were considered as 0.90504m and 0.736m/s, respectively. The comparison of measured water depth obtained from DID with simulated water depth from LABSWE™ are plotted, as shown in Figure 14.

From the validation test, the percentage difference between measured and simulated water depths are 1.93, 1.23 and 1.56% for 2017, 2016 and 2015, respectively.

TABLE 4. Input parameters for simulating water depth for year 2015

Parameters	Value
No. of lattices in x-direction, L_x	559
No. of lattices in y-direction, L_y	109
Initial water depth, h	0.90504m
Initial flow velocity, u	0.736m/s
Time step, Δt	0.0005s
Relaxation time, τ	1.0
Lattice size in x-direction, Δx	0.5m
Lattice size in y-direction, Δy	0.5m

**Figure 14.** Cross-section of simulated against measured water depth for year 2015

The small differences indicate that the model is capable of simulating potential headwater accidents at Lata Kinjang waterfall. In addition, according to Zhou [31], the LBM may result in numerical instability during the simulation, which potentially contributes to the slight percentage difference. However, the stability condition is expected to be achieved when the kinematic viscosity, ν is positive, the magnitude of celerity is lesser than 1 and the shallow water flow condition is subcritical.

The numerical simulation of a headwater accident at Lata Kinjang waterfall is initialized by dividing the model into two parts in terms of L_x . A higher water height of 2.1 m is assigned from $L_x=1$ to $L_x=20$. The L_x range of 1 to 20 is determined based on size of the basin of Lata Kinjang waterfall. The high-water height is selected based on the maximum capacity of the basin of Lata Kinjang waterfall. On the other hand, L_x range of 21 to 559 is inputted with a water height of 0.9 m based on the assumption that the channel is in normal flow condition. According to data reported by Adegoke et al. [34], in terms of water velocity, the initial velocity of the basin ($L_x=1$ to 20) is set at 10m/s. The usual flow velocity of 0.736m/s is inputted for downstream of the channel ($L_x=21$ to 559). The input parameters for the numerical computation are presented in Table 5. Results from the simulation of headwater accident in Lata Kinjang waterfall are represented in terms of water level progression along the channel from $t=0$ s to $t=72$ s and velocity profiles of $t=0$ s to $t=12.5$ s.

As observed from the water height progression in Figures 12 to 14, water height from the basin area ($L_x=1$ to 20) gradually decreased. However, from water depth, $L_x=21$, the water height of downstream begins to increase, indicating that a high quantity of water from upstream surges downstream which consistent with the occurrence of a headwater accident. Also, from $L_x=131$ there is a water level decrease until a minimum level of 0.72 m is reached at $L_x=171$. This reduction is attributable to changes in bed slope from gentle to steeper zone. Conversely, water height is observed to increase at $L_x=311$ and $L_x=454$ due to the cascading of water from steeper to gentle slopes. Basically, the pull of gravitational force is stronger when water flows down a steeper bed

TABLE 5. Input parameters for headwater accident in Lata Kinjang Waterfall

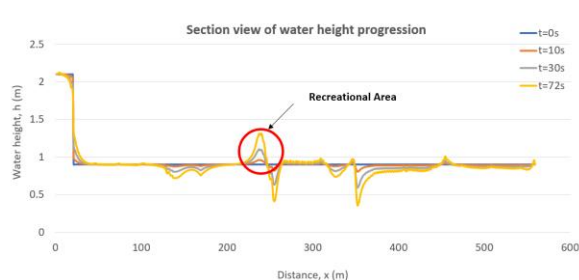
Parameters	Value
No. of lattices in x-direction, L_x	559
No. of lattices in y-direction, L_y	109
Initial water depth from $L_x=1$ to $L_x=20$, h_1	2.1m
Initial water depth from $L_x=21$ to $L_x=559$, h_2	0.9m
Initial flow velocity from $L_x=1$ to $L_x=20$, u_1	10m/s
Initial flow velocity from $L_x=21$ to $L_x=559$, u_2	0.736m/s
Time step, Δt	0.0001s
Relaxation time, τ	1.0
Lattice size in x-direction, Δx	0.5m
Lattice size in y-direction, Δy	0.5m

slope. Subsequently, water velocity increases, while water height decreases.

Furthermore, fluctuations in water height become delineated from $L_x=213$ to $L_x=262$, and partly from $L_x=317$ to $L_x=444$ as displayed in Figure 13. These water height fluctuations result from changes in channel shape. The areas near the edge of the channel were the ones modeled. Therefore, the high-water level contributes to the fluctuations by providing higher friction at the edge of the channel. In this situation, water molecules are slowed down by the edge of the channel, leading to a higher water level. Nonetheless, the lower water level in the referred areas reflects the flow of water to a wider area, which accounts for the increase in velocity.

With regards to the recreational area of Lata Kinjang waterfall, which is located from $L_x=205$ to $L_x=238$, the simulated water height rises up to 45% with a maximum water level of 1.31m. Therefore, the recreational area of Lata Kinjang waterfall can be considered highly susceptible to headwater accident.

The water velocity profiles at $t=0s$ and $t=12.5s$ are illustrated in Figures 16 and 17, respectively. As observed, high water velocity in the upstream area ($L_x=1$ to $L_x=20$) increases the water velocity in the

**Figure 15.** Graph of water height progression against the distance along Lata Kijang waterfall for $t = 0s, 10s, 30s$ and $72s$

downstream area (from $L_x=21$). Nonetheless, the maximum water velocity in downstream is 0.3388m/s at $t=12.5s$, which is relatively low compared to similar studies conducted. This may due to assumed relaxation time of 1 that was inputted into the simulation to stabilize the model. In addition, the relaxation time, τ correlates with the kinematic viscosity, ν , which is expressed in Equation (8) [31].

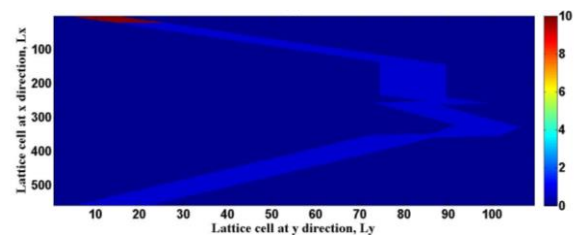
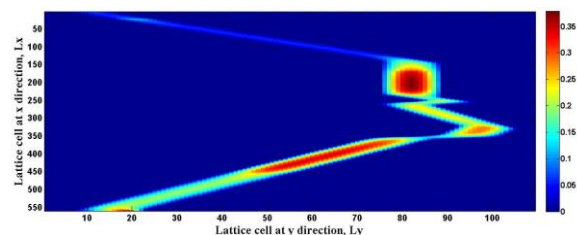
$$\nu = \frac{e^2 \Delta t}{6} (2\tau - 1) \quad (8)$$

By using Equation (8), the kinematic viscosity of water from the simulation is calculated as $16.667m^2/s$, which is comparatively higher than the usual water kinematic viscosity of $0.801 \times 10^{-6}m^2/s$ at $30^\circ C$ [35]. Since water velocity and kinematic viscosity have an inverse relationship, the difference in the kinematic viscosity led to lower water velocity in the simulation results.

In spite of the low water velocity, the water velocity profile from Figure 17 indicates that the recreational area ($L_x=205$ to $L_x=238$) will be influenced by the high water velocity.

To prevent or reduce the impact of headwater accident in Lata Kinjang waterfall, some solutions are suggested. Firstly, it is advised that the bed slope of the Lata Kinjang waterfall has to be modified into a gentler slope, especially in the recreational area. Since the gravitational force is weaker in a gentle slope, the velocity of water flowing down will be lower. The lower water velocity will then reduce the impact of water flow during headwater accidents. Furthermore, the bed slope can be maintained at 0.2182 along the channel to decrease the possibility of water level difference.

Secondly, hard protection structures such as revetment can be constructed at the edges of the channel, particularly for the areas of $L_x=213$ to $L_x=262$ and $L_x=317$ to

**Figure 16.** Water velocity profile at $t=0s$ **Figure 17.** Water velocity profile at $t=12.5s$

$L_x=444$. It is expected that the destruction of the bank of flow channel due to high water level can be minimized with the aid of hard protection structures. However, the aesthetics of the surrounding should be taken into consideration during the construction due to the fact that Lata Kinjang waterfall is a tourist attraction spot.

Finally, government bodies should monitor the basin of Lata Kinjang waterfall regularly to envisage potential occurrences of headwater accidents. Objects such as rocks and logs that interrupt the water flow shall be removed from the basin. With the scheduled removal of blockage objects in the basin, the possible occurrence of headwater accidents will be averted or lessened to a minimum.

5. CONCLUSIONS

This research simulated the potential occurrence of headwater accidents at Lata Kinjang waterfall using the LABSWETM model. The results were validated with data obtained from Department of Irrigation and Drainage (DID), Malaysia. The validation procedure showed an average percentage error of 1.57%, which confirms the capability of the model to simulate potential headwater accidents in the study area. Results from the computational simulation were presented in terms of water height progression from $t=0s$ to $t=72s$ and water velocity profile at $t=0s$ and $t=12.5s$. The results indicated that the recreational area of Lata Kinjang waterfall will be highly impacted by the occurrence of a headwater accident due to increase in water level and velocity. It is apparent from the simulation results that the flow of potential headwater accident is influenced by the steepness of bed slope, edges of the channel and shape of the channel. Hence, this study proposes specific steps to mitigate possible headwater accidents, and they include: modification of the bed slope to a gentler one especially in the recreational area; construction of hard protection structures such as revetment at the edges of the channel, particularly for the areas of high water velocities ($L_x=213$ to $L_x=262$ and $L_x=317$ to $L_x=444$) to prevent destruction of the channel bank, and regular monitoring and maintenance of the waterfall by appropriate government bodies. For further development of this research, it is suggested to study the interaction of headwater with objects in the river which can be investigated by integrating the present model in this study with a conventional numerical method such as Finite Volume Method (FVM).

6. REFERENCES

1. Lowe, W. H. and Likens, G. E., "Moving headwater streams to the head of the class", *BioScience*, Vol. 55, (2005), 196-197.
2. Butman, D., Stackpoole, S., Stets, E., McDonald, C. P., Clow, D. W. and Striegl, R. G., "Aquatic carbon cycling in the conterminous United States and implications for terrestrial carbon accounting", *Proceedings of the National Academy of Sciences*, Vol.113, (2016), 58-63.
3. Marx, A., Dusek, J., Jankovec, J., Sanda, M., Vogel, T., Van Geldern, R., Hartmann, J. and Barth, J. A. C., "A review of CO₂ and associated carbon dynamics in headwater streams: A global perspective", *Review of Geophysics*, Vol. 55, (2017), 560-585.
4. United Press International. (2004). Seven injured at Malaysia waterfall. Retrieved 2017, 7th October from <https://www.upi.com/Seven-injured-aty-Malaysiawaterfall/22431104022079/?spt=su>
5. Naluri Bangsa. (2017). Remaja lemas dihanyut kepala air di Kg. Sungai Bil Behrang. Retrieved 2017, 9th October from <http://naluribangsa.com/web/remaja-lemasdihanyut-kepala-air-di-kg-sungai-bil-behrang/>
6. Ali, A., Pasha, G. A., Ghani, U., Ahmed, A. and Abbas, F. M., "Investigating Role of Vegetation in Protection of Houses during Floods", *Civil Engineering Journal*, Vol. 5, (2019), 2598-2613.
7. Gharib, M., Motamedvaziri, B., Ghermezcheshmeh, B. and Ahmadi, H., "Calculation of the Spatial Flooding Intensity with Unit Flood Response Method in the Tangrah Watershed, Iran", *Civil Engineering Journal*, Vol. 3, (2019), 1327. DOI : 10.28991/cej-2019-03091436
8. S. Giertz, B. Diekkrüger, G. Steup, "Physically-based modeling of hydrological processes in a tropical headwater catchment (West Africa)-process representation and multi-criteria validation", *Hydrology and Earth System Sciences Discussions*, Vol. 10, (2006), 829-847.
9. Voltz, T., Gooseff, M., Ward, A. S., Singha, K., Fitzgerald, M. and Wagener, T., "Riparian hydraulic gradient and stream-groundwater exchange dynamics in steep headwater valleys", *Journal of Geophysical Research: Earth Surface*, Vol. 118, (2013), 953-969.
10. Voekler, H. M., Allen, D. M. and Alila, Y., "Modeling coupled surface water-Groundwater processes in a small mountainous headwater catchment", *Journal of Hydrology*, Vol. 517, (2014), 1089-1106.
11. Kelleher, C., Wagener, T. and McGlynn, B., "Model-based analysis of the influence of catchment properties on hydrologic partitioning across five mountain headwater subcatchments", *Water Resources Research*, Vol. 51, (2015), 4109-4136.
12. Niu, J., Chen, J., Wang, K. and Sivakumar, B., "Multi-scale streamflow variability responses to precipitation over the headwater catchments in southern China", *Journal of Hydrology*, Vol. 551, (2017), 14-28.
13. Li, W., Zhang, K., Long, Y. and Feng, L., "Estimation of Active Stream Network Length in a Hilly Headwater Catchment Using Recession Flow Analysis", *Water*, 2017, Vol. 9, (2017), 348. <https://doi.org/10.3390/w9050348>
14. Neupane, R. P., Adamowski, J. F., White, J. D. and Kumar, S., "Future streamflow simulation in a snow-dominated Rocky Mountain headwater catchment", *Hydrology Research*, Vol. 49, (2018), 1172-1190.
15. Allen, G. H., Pavelsky, T. M., Barefoot, E. A., Lamb, M. P., Butman, D., Tashie, A. and Gleason, C.J., "Similarity of stream width distributions across headwater systems", *Nature Communications*, Vol. 9, (2018), 610. <https://doi.org/10.1038/s41467-018-02991-w>
16. Aidun, C. K. and Clausen, J.R., "Lattice-Boltzmann method for complex flows", *Annual Review of Fluid Mechanics*, Vol. 42, (2010), 439-472.
17. Zhou, J. G., "A lattice Boltzmann model for the shallow water equations", *Computer Methods in Applied Mechanics and Engineering*, Vol. 191, (2002), 3527-3539.
18. Qiu, L. C., Tian, L., Liu, X. J. and Han, Y., "A 3D multiple-relaxation-time LBM for modeling landslide-induced tsunami waves", *Engineering Analysis with Boundary Elements*, Vol. 102, (2019), 51-59.

19. Hedjripour, A. H., Callaghan, D. P. and Baldock, T. E. , "Generalized transformation of the lattice Boltzmann method for shallow water flows", *Journal of Hydraulic Research*, Vol.54, (2016), 371-388.
20. Dolanský, J., Chára, Z., Vlasák, P. and Kysela, B., "Lattice Boltzmann method used to simulate particle motion in a conduit", *Journal of Hydrology and Hydromechanics*, Vol. 65, (2017), 105-113.
21. Mousavi, T. S., Sedighi, K., Farhadi, M. and Fattahi, E., "Lattice Boltzmann simulation of deformation and breakup of a droplet under gravity force using interparticle potential model", *International Journal of Engineering, Transactions A: Basics*, Vol. 26, (2013), 781-794.
22. Sheikholeslami, M. and Ashorynejad, H. R., "Lattice boltzmann simulation of nanofluids natural convection heat transfer in concentric annulus", *International Journal of Engineering, Transactions B: Application*, Vol. 26, (2013), 895-904.
23. Galina, V., Cargnelutti, J., Kaviski, E., Gramani, L. M. and Lobeiro, A. M., "Application of lattice boltzmann method for surface runoff in watershed", *Revista Internacional de Métodos Numéricos para Cálculo y Diseño en Ingeniería*, Vol. 34, (2018). <https://doi.org/10.23967/j.rimni.2017.6.001>
24. Li, S., Li, Y., Zeng, Z., Huang, P. and Peng, S., "An evaluation of force terms in the lattice Boltzmann models in simulating shallow water flows over complex topography", *International Journal for Numerical Methods in Fluids*, Vol. 90, (2019), 357-373.
25. Peng, Y., Zhang, J. M. and J.G. Zhou, "Lattice boltzmann model using two relaxation times for shallow-water equations", *Journal of Hydraulic Engineering*, Vol. 142, (2015), 06015017. [https://doi.org/10.1061/\(ASCE\)HY.1943-7900.0001065](https://doi.org/10.1061/(ASCE)HY.1943-7900.0001065)
26. Sato, K., Adriano, B. and Koshimura, S., "A Precise Tsunami numerical analysis of lattice botzmann method focusing on the external force term", *Journal of Japan Society of Civil Engineers*, Ser. B3 (Ocean Engineering), Vol. 72, (2016), I-145-I-150.
27. Wang, H., Cater, J., Liu, H., Ding, X. and Huang, W., "A lattice Boltzmann model for solute transport in open channel flow", *Journal of hydrology*, Vol. 556, (2018), 419-426.
28. Zergani, S., Aziz, Z. A. and Viswanathan, K. K., "A shallow water model for the propagation of tsunami via Lattice Boltzmann method", in 2nd International Conference on Geological, Geographical, Aerospace and Earth Sciences 2014, *IOP Conference Series: Earth and Environmental Science*, Bali, Indonesia, Vol. 23, 012007, (2015). <https://doi.org/10.1088/1755-1315/23/1/012007>
29. Zhang, X., Feng, J. and Yang, T., "Lattice Boltzmann method for overland flow studies and its experimental validation", *Journal of Hydraulic Research*, Vol. 53, (2015), 561-575.
30. Zhao, Z. M., Huang, P. and Li, S. T., "Lattice Boltzmann model for shallow water in curvilinear coordinate grid", *Journal of Hydrodynamics*, Vol. 29, (2017), 251-260.
31. Zhou, J. G., "Lattice Boltzmann methods for shallow water flows", Springer, Berlin, Vol. 4, (2004). <https://doi.org/10.1007/978-3-662-08276-8>
32. Shafiai, S. H., Shahrzuzaman, D. B., Goh, J. X., and Latheef, M., "Lattice Boltzmann Method of a Flooding Accident at Gopeng, Perak, Malaysia", *Mathematical Problems in Engineering*, (2017), Article ID 3478158, <https://doi.org/10.1155/2017/3478158>
33. Day, M. A., "The no-slip condition of fluid dynamics", *Erkenntnis*, Vol. 33, (1990), 285-296. <https://doi.org/10.1007/BF00717588>
34. Adegoke, P. B., Atherton, W., and Al Khaddar, R. M., "A novel simple method for measuring the velocity of dam-break flow", *WIT Transactions on Ecology and the Environment*, Vol. 184, (2014), 23-34.
35. Engineers Edge. 2018. Retrieved 2018, 30th March from https://www.engineersedge.com/physics/water_density_viscosity_specific_weight_13146.htm.

Persian Abstract

چکیده

انباشت اتفاقی آب در بالا دست رودخانه یک پدیده ی طبیعی است که امکان وقوع پیوستن آن در هر کانال جریان وجود دارد و باعث بروز خسارات عظیمی، شامل آسیب رساندن به محیط زیست اطرافش است. ماین مطالعه، امکان شبیه سازی پدیده ی انباشت اتفاقی آب در بالا دست آبشار لاتاکیجنگ در استان پراک واقع در کشور مالزی را مورد بررسی قرار داده است. ماین حادثه با استفاده از روش مشبک بولتزمن با هدف درک رفتار این گونه صوانج از منظر هیدرولیکی مورد مطالعه قرار گرفته است. برای بررسی شرایط آبشار مورد مطالعه، یک شبیه سازی دو بعدی با استفاده از روش شبکه ی بولتزمن برای جریان آب کم عمق با مدل سازی آشفستگی انجام شده است. نتایج حاصل از شبیه سازی از نظر پیشرفت ارتفاع آب و مشخصات سرعت ارائه شده است. نتایج حاصل از ارتفاع آب، به ترتیب کاهش و افزایش در حوزه و پایین دست را نشان داد، و نتایج پروفایل سرعت بیانگر افزایش سرعت در پایین دست بود. بنابراین، این، شرایط فعلی آبشار لاتاکیجنگ به شدت مستعد این گونه حوادث است. چندان راه کار ممکن برای کاهش مؤثر این پدیده ارائه شده است.
